Investigation of the Flame Structure of Spray-A Using the Transported Probability Density Function

M. A. Chishty[1], Y. Pei[2], E. R. Hawkes[1,3], M. Bolla[1] and S. Kook[1]

[1]School of Mechanical & Manufacturing Engineering,
University of New South Wales, Sydney 2052, Australia

[2]Energy System Division, Argonne National Laboratory, Argonne, IL 60439, USA

[3]School of Photovoltaic and Renewable Energy Engineering,
University of New South Wales, Sydney 2052, Australia

Abstract

An *n*-dodecane spray (Spray A) injected into a high-pressure and high-temperature combustion vessel at typical diesel engine conditions is investigated using the transported probability density function (TPDF) method. The Lagrangian Monte Carlo method is used to treat the TPDF equation. The unsteady Reynolds averaged Navier-Stokes (URANS) k-ε turbulence model is used to provide the turbulence information to the TPDF solver. The micro-mixing term is closed by the Euclidean minimum spanning trees (EMST) model. A reduced chemical mechanism with 88 species is implemented. The spray is treated by a traditional Lagrangian discrete phase model. The cool flame structure (CH_2O) together with the high temperature reaction zone (OH) are examined at different ambient temperatures and ambient oxygen conditions, and compared with the available experimental results from 355 nm planar laser-induced fluorescence (PLIF) and OH PLIF. A good agreement has been found for some of these measurements, while agreement for others leaves room for improvement.

Introduction

In addition to the wide spread use of compression ignition (CI) engines for heavy-duty and marine engines, CI engines are also becoming of increasing interest for passenger car propulsion due to their high thermal efficiency. However, conventional diesel engines emit high levels of pollutants, such as NO_x and soot. Therefore, advanced strategies such as lower temperatures, higher pressures, multiple fuel-injections, exhaust gas recirculation (EGR) and alternative fuels [1, 2] are being used for in the development of clean and efficient CI engines. The increased predictive capability of computational fluid dynamics (CFD) models is becoming a valuable tool for this advanced technology. These CFD models have to deal with multiple combustion modes under high Weber number spray, high Reynolds number turbulence and complex chemical kinetics.

Many complexities are involved when it comes to the modelling of practical diesel spray combustion such as finite-rate chemistry and dealing with multi modal combustion (i.e., non-premixed and premixed) in the same flame [1]. Most related research is being done using the well-mixed model which assumes that the thermochemical states have no turbulent fluctuations [3-6]. In the 90's, advanced turbulent combustion theories started to appear with different turbulence-chemistry interaction (TCI) approaches, e.g., flamelet models [7-8], conditional moment closure [9-11] and TPDF methods [12-16].

The TPDF model has several advantages for modelling diesel spray flames: i) the chemical source term appears in closed form, which is particularly useful for fundamentally transient problems that involve both fast and slow dynamics, ii) the method does not assume a specific state of reactant mixedness, which is important since both premixed and non-premixed combustion occurs, iii) it does not assume the thermochemical state lies on any particular low-dimensional manifold, e.g. one parameterised only by mixture-fraction, and iv) it does not assume any particular form for scalar PDFs. It is found in the literature that the method has performed well for the applications of diesel jet flame [12-16].

The objective of this paper is to compare the computed results of flame structure from the TPDF approach with recent experimental measurements using 355 nm PLIF and schlieren imaging from Ref. [17] performed in the context of the Engine Combustion Network (ECN) [18]. Computed flame structures are explored at different ambient temperatures and ambient oxygen conditions and their impact on the distribution of CH_2O, OH, OH* and C_2H_2 species is discussed in detail.

Methodology

Turbulence and Combustion Models:

The present study was conducted on ANSYS FLUENT 14.5 finite volume based CFD commercial code along with its pre-processor Gambit. The TPDF model is coupled with an unsteady, Reynolds averaged Navier-Strokes (RANS) k-ε turbulence model for which implementation details can be found in Ref. [19]. An analysis of the sensitivity to the turbulence model constant $c_{\epsilon 1}$ was investigated in [20] and $c_{\epsilon 1} = 1.50$ is used for the current study. The unclosed molecular mixing is modelled using the EMST model. Turbulent transport is modelled by the gradient diffusion hypothesis.

The approach selected to solve the TPDF equations is the Lagrangian Monte Carlo method due to its ability of dealing with the high dimensionality complication [15]. In this approach, the computational domain was filled with notional particles, which discretely represent the flow field. Each notional particle has a probability weight, and carries composition and enthalpy. The finite volume solver takes the feedback from the PDF solver, i.e. the mean density which was used to solve the momentum and turbulence model equations in the finite-volume side. A reduced *n*-dodecane chemical mechanism with 88 species has been used [16]. The in-situ adaptive tabulation (ISAT) scheme was implemented to accelerate the chemistry calculation and simulations were carried out on 64 processors.

Computational Setup:

The numerical setup is summarised in Table 1. The unsteady pressure-based solver was employed. The "standard" discretisation was applied for pressure, and SIMPLE was used for the pressure-velocity coupling. The convective terms were

discretised using a first order upwind scheme. Further description of these models is available in the FLUENT user guide [20]. A simple group injection method is used and the injection parameters are shown in Table 2.

To model the constant volume chamber, a 2D axi-symmetric computational grid was selected having dimensions of 100×63 mm and a total number of cells of 2300. The convergence studies of mesh, time step size, number of particles per cell and ISAT error tolerance have been conducted in previous studies [16, 21]. Test cases considered in this study are summarized in Table 3. Case 1 is the reference case, for which experimental data from Ref. [17] were available.

Numerical setup	
Domain	2D axi-symmetric
Solver	Unsteady pressure based
Turbulence model	Standard $k - \epsilon$ model with $c_\mu = 0.09$, $c_{\epsilon 1} = 1.50$, $c_{\epsilon 2} = 1.92$, $\sigma_k = 1.0$, $\sigma_t = 1.3$, $\sigma_\emptyset = 1$
Mixing model	EMST, $c_\emptyset = 1.5$
Discretisation scheme	Standard for pressure, SIMPLE for pressure-velocity coupling, 1st order upwind on momentum, k, ϵ and density

Table 1. Numerical setups for the reacting cases.

Injection profile setup	
Fuel density	713 kg/m^3
Ambient density	22.8 kg/ m^3
Fuel temperature	363 K
Orifice diameter	0.09 mm
Injection velocity	650.77 m/s
Injection duration	6 ms

Table 2. Injection parameters.

Test cases			
Case	Temperature (K)	Oxygen (mole %)	Ambient Pressure (MPa)
1	900	15	5.94
2	800	15	5.25
3	1000	15	6.62
4	900	13	5.94
5	900	21	5.94

Table 3. Test cases performed for the variations of temperature and ambient oxygen at 150 MPa injection pressure.

Results and Discussions

In this section, a detailed analysis of the flame structure is presented. To date, the experimental data of 355 nm PLIF and schlieren images were not available for injector 677 (IFPEN). Therefore, a different injector 370 (SANDIA) [22] is used in this study for the direct comparison for case 1 (see Table 3). Experimental data is selected at 1.69 ms [17] and compared with simulation results at 1.7 ms as illustrated in Figure 1. In the images, the fuel is injected vertically. From left to right: (a) experimental 355nm LIF, (b) computed mass fraction of acetylene (C_2H_2, left) and formaldehyde (CH_2O, right), (c) experimental schlieren image and (d) computed mass fraction of hydroxyl radical in its excited (OH*, left) and ground state (OH, right). In the computed fields (b and d), the yellow and white lines represent iso-contours of mean mixture fraction values of 0.01 and stoichiometric (0.045), respectively. The yellow line is a marker of the spray boundary and is compared with the boundary of the schlieren image. The white line is a marker for the high temperature region and discriminates the mean fuel rich from the mean fuel lean region. It is noted that, the injector 370 and its rate of injection [22] is only used for the comparison of experimental and numerical results illustrated in Figure 1.
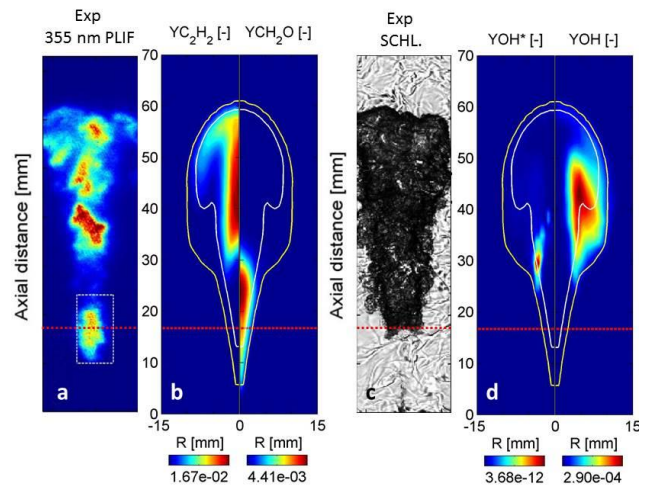

Figure 1. Contour plots of CH₂O, OH * and OH mass-fraction between experiments and simulations at 1.69 ms for test case 1 [17].
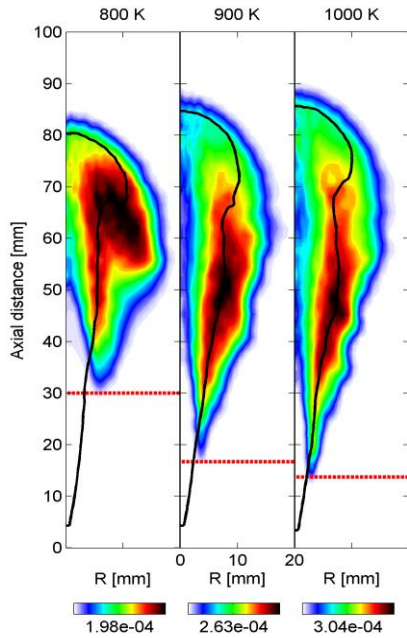
The experimental 355nm PLIF measures CH_2O in the near field of the jet and polycyclic aromatic hydrocarbons (PAH) in the downstream region. One can compare the PAH with C_2H_2 mass fraction, as acetylene is the building block of soot or PAH and is routinely employed as a soot precursor in semi-empirical soot models. Also, because PAH have not been included in the current simulation. The location of C_2H_2 mass fraction is well captured by the simulation; while an over-prediction of few millimetres has been noticed for formaldehyde (see Fig. 1 (a and b)). The reason might be the difference in injector as well as the injection duration. Other reason could be that the location of formaldehyde is strongly dependent on the ambient temperature and 10 to 40K ambient temperature differences can play a major role. As no direct comparison is currently available for injector 677 (IFPEN), it is therefore hard to draw any conclusion on that point. However, the location of formaldehyde is close to the injector tip, which means that low-temperature regions occur close to the injector. On the other half of Figure.1 (c) and (d), the lift-off length (LOL) can be visualized in the schlieren images (i.e., red dashed lines). In the simulation, the LOL is defined as the minimal axial distance from the injector tip where 14% of the domain maximal value of OH mass fraction is found. This definition was found to be equivalent to a 50% levelling-off value of OH* chemiluminescence. The LOL is well-predicted by the numerical simulation, i.e., 16.72 mm, while the experimental value for the current case is 16.7 mm. The yellow line (i.e. spray boundary) also provides the reactive spray length, which is in a good agreement with the experimental data. At 1.69 ms, the reported experimental value of the axial spray extent is 61.5 mm, while it is 62 mm for the numerical simulations.

The effects of the ambient temperature on OH and CH_2O mass fractions have been explored numerically at 4 ms and are shown in Figure 2. The black line shows the stoichiometric mixture fraction, while the red dashed line represents the computed LOL. Figure 2 (a) shows that the high temperature reaction zone is stretched and the magnitude increases with the increase in ambient temperature. However, the region of cool flame gets compact at higher ambient temperature conditions as presented in Figure 2 (b). For the 800K case, the mass fractions of OH and CH_2O are approximately a factor of 1.8 and 1.3 lower compared to those of the1000K case, respectively. The axial starting point of formaldehyde is similar for all cases 1, 2 and 3, i.e. axially 10 mm. Higher width of CH_2O field has been observed at the low temperature and vice versa. The ambient temperature has an
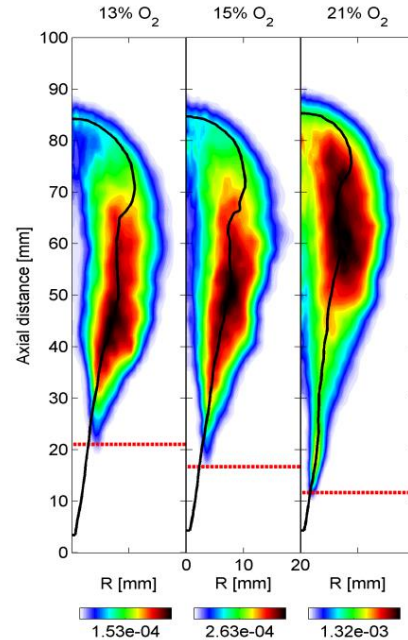
effect on the location of high temperature reaction zones and the width of the cool flame regions.

The pictorial view of the mass fractions of OH and CH$_2$O for different ambient oxygen conditions is shown in Figure 2 (c) and (d), respectively. The magnitude of the OH mass fraction is highly dependent upon the ambient oxygen. The value of 13% O$_2$ case is a f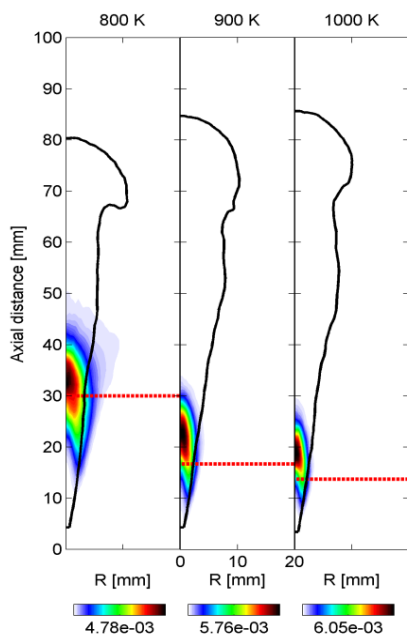actor of 1.8 and 9 smaller compared to the 15 % and 21% O$_2$, respectively. On the other hand, the width of CH$_2$O region does not change appreciably with variations in ambient oxygen. However, the intensity of 13% O$_2$ is almost double in comparison with that of 21% O$_2$. The variation of ambient oxygen has a strong impact on the magnitude of OH mass fraction, but small impact on the width and magnitude of the CH$_2$O region.
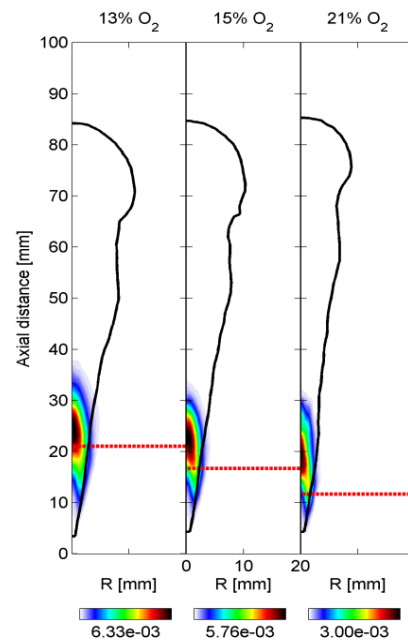

(a) OH mass fraction at 800, 900, 1000K

(b) OH mass fraction at 13, 15 and 21% O$_2$

(c) CH$_2$O mass fraction at 800, 900 and 1000K

(d) CH$_2$O mass fraction at 13, 15 and 21% O$_2$

Figure 2. Computed fields of mean mass fraction of OH and CH$_2$O at 4 ms after start of injection. The black iso-contours represent the mean stoichiometric mixture fraction. The red dashed lines correspond to the computed LOL. For all cases, numbers drawn below the colourbars are the maximal scale values and minimal values are zero.

Conclusions

An *n*-dodecane spray has been modelled at diesel engine conditions by treating the continuous phase with the TPDF approach and the liquid spray with the Lagrangian discrete phase model. An 88 species reduced chemical mechanism was used to explore the high temperature reaction zones and cool flame structures at different ambient temperatures and ambient oxygen conditions. It was demonstrated that the location and flame structures of formaldehyde- and PAH-PLIF and schlieren images are well predicted in comparison with the experimental data. However, possibly due to differences between injectors and injection duration, the over-prediction of few millimetres has been noticed in the axial location of formaldehyde. On the other hand, the LOL and the flame length are in a good agreement with the experimental data.

The ambient temperature has an effect on the location of high temperature reaction zones and the width of the cool flame structure. For the 800 K case, the mass fractions of OH and CH_2O are roughly a factor of 1.8 and 1.3 compared to those of 1000 K case, respectively. On the other hand, the variation of ambient O_2 affects the intensity of OH and CH_2O mass fractions, rather than its location and width.

Acknowledgments

References

[1] Dec, J.E., Advanced compression-ignition engines-understanding the cylinder processes, *Proc. Combust. Inst.*, **32(2)**, 2009, 2727-2742.

[2] Reitz, R.D., Directions in internal combustion engine research, *Combust. Flame.*, **160**, 2013, 1-8.

[3] D'Errico, G., Ettorre, D., and Lucchini, T., Simplified and detailed chemistry modelling of constant-volume diesel combustion experiments, *SAE Int. J. Fuels Lubr.*, **1(1)**, 2009, 452-465.

[4] Vishwanathan, G., and Reitz, R.D., Development of a practical soot modelling approach and its application to low-temperature diesel combustion, *Combust. Sci. Tech.*, **182(8)**, 2010, 1050-1082.

[5] Som, S., and Aggarwal, S. K., Effects of primary breakup modelling on spray and combustion characteristics of compression ignition engines, *Combust. Flame.*, **157(6)**, 2010, 1179-1193.

[6] Pei, Y., Hawkes, E., and Kook, S., Modelling *n*-heptane spray and combustion in conventional and low-temperature diesel engine conditions, in *Proceedings of the Australian Combustion Symposium 2011*, AU., 2011, 90-93.

[7] Bekdemir, C., Somers, L. M. T., deGoey, L.P.H., Tillou, J., and Angelberger, C., Predicting diesel combustion characteristics with large-eddy simulations including tabulated chemical kinetics, *Proc. Combust. Inst.*, **34(2)**, 2013, 3067-3074.

[8] Kundu, P., Pei, Y., Wang, M., Mandhapati, R., and Som, S., Evaluation of turbulence-chemistry interaction under diesel engine conditions with multi-flamelet RIF model, *Atomizat. Spray*, **24(9)**, 2014.

[9] Borghesi, G., Mastorakos, E., Devaud, C. B., and Bilger, R.W., Modelling evaporation effects in conditional moment closure for spray autoignition, *Combust. Theory Model.*, **15(5)**, 2001, 725-752.

[10] Bolla, M., Wright, Y. M., Boulouchos, K., Borghesi, G., and Mastorakos, E., Soot formation modelling of *n*-heptane sprays under diesel engine conditions using the conditional moment closure approach, *Combust. Sci. Tech*, **185**, 2013, 766-793.

[11] Bolla, M., Farrace, D., Wright, Y. M., Boulouchos, K., and Mastorakos, E., Influence of turbulence–chemistry interaction for *n*-heptane spray combustion under diesel engine conditions with emphasis on soot formation and oxidation, *Combust. Theory Model.*, **18(2)**, 2014, 330-360.

[12] Bhattacharjee, S., and Haworth, D.C., Simulations of transient *n*-heptane and *n*-dodecane spray flames under engine-relevant conditions using a transported PDF method, *Combust. Flame.*, **160(10)**, 2013, 2083-2102.

[13] Mohan, V.R., and Haworth, D.C., Turbulence-chemistry interactions in a heavy-duty compression-ignition engine, in *Proceedings of the Combustion Institute 2014*, 2014, in press.

[14] Pei, Y., Hawkes, E., and Kook, S., Transported probability density function modelling of the vapour phase of an *n*-heptane jet at diesel engine conditions, *Proc. Combust. Inst.*, **34**, 2013, 3039-3047.

[15] Pei, Y., Hawkes, E., and Kook, S., A comprehensive study of effects of mixing and chemical kinetic models on predictions of *n*-heptane jet ignitions with the PDF method, *Flow Turb. Combust.*, **91(2)**, 2013, 249-280.

[16] Pei, Y., Hawkes, E.R., Kook, S., Goldin, G.M. and Lu, T., Modelling *n*-dodecane spray and combustion with the transported probability density function method, *Combust. Flame*, submitted, 2014.

[17] Skeen, S. A., Manin, J., and Pickett, L. M., Simultaneous formaldehyde PLIF and high-speed schlieren imaging for ignition visualization in high-pressure spray flames, *Proc. Combust. Inst.*, In press, 2014.http://dx.doi.org/10.1016/j.proci.2014.06.040

[18] Pickett, L.M., Bruneaux, G. and Payri, R., Engine Combustion Network, http://www.sandia.gov/ecn/index.php.

[19] Pope, S.B., PDF methods for turbulent reactive flows, *Prog. Energy Combust. Sci.*, **11**, 1985, 119-192.

[20] ANSYS. *FLUENT 14.5 Theory Guide*, ANSYS Inc., 2012

[21] Pei, Y., Transported PDF modelling of spray combustion at practical diesel engine conditions, *PhD thesis.*, School of Photovoltaic and Renewable Energy Engineering, UNSW, Australia, April, 2013.

[22] http://www.sandia.gov/ecn/cvdata/sandiaCV/injectorCharacterization-2007.php